SUPPLEMENTAL MATERIAL

Experimental Procedures

Steady-state anisotropy of DPH incorporated in KRMs- For the incorporation of 1,6-diphenyl-1,3,5-hexatriene (DPH) into KRMs, 0.5 µl of a 100 µM DPH (dissolved in dimethylformamide) solution was added to 200 µl of KRMs (20 eq.) in buffer H. These conditions kept the amount of organic solvent added to the KRMs to a minimum (0.25 % of final volume). The KRM-DPH mixture was incubated for 1 h at 4ºC in the dark to prevent any photodegradation of the fluorescent probe. Thereafter, the KRMs were collected by sedimentation through a 0.5 M sucrose cushion in buffer H (Beckman TLA100 rotor; 100,000 rpm: 5 min; 4ºC) and the KRM pellet was resuspended in 300 µl of buffer H. The samples were then incubated for at least 10 min at the indicated temperature, and the steady-state anisotropy (r; λ_{ex}=350 nm; λ_{em}=452 nm; both with a 4 nm bandpass) of DPH in KRMs was measured as before (1). To obtain the net DPH emission intensities, the component intensities of an equivalent DPH-free KRM sample were subtracted from the corresponding component intensities of a DPH-containing KRM sample. Since DPH and its derivatives are essentially nonfluorescent in an exclusively aqueous environment (2), the anisotropy of unincorporated DPH in a KRM-free sample was determined using methanol as solvent.

Liposome preparation- Liposomes containing 100 mol% 1-palmitoyl-2-oleoyl-*sn*-glycero-3-phosphocholine (POPC) or 25 mol% 1-palmitoyl-2-oleoyl-*sn*-glycero-3-[phospho-L-serine] (POPS) / 75 mol% POPC were prepared as before (3) and are designated PC for 100 mol% POPC, and PCPS for 75 mol% POPC, 25 mol% POPS. For use in lipophilic quenching experiments, they were prepared as above, except that 10, 20, or 30 mol% of the POPC was replaced by the nitroxide-labeled phospholipid 1-palmitoyl-2-stearoyl-(x-doxyl)-*sn*-glycero-3-phosphocholine (xNOPC, where x is equal to 5 or 12 and indicates the acyl chain carbon to which the NO moiety is covalently attached) to yield a final total NOPC concentration of 7.5, 15, or 22.5 mol%, respectively. The vesicles contain POPS, POPC, and NOPC, but are designated either 5NOPC or 12NOPC. All phospholipids were obtained from Avanti Polar Lipids (Alabaster, AL).

Collisional quenching of NBD emission intensity by iodide ions- $RTA^{259\text{-}NBD}$ (450 nM) and KRMs (80 eq) or an equal volume of microsome buffer were combined in 1200 µl buffer H, after which four equal aliquots of the mixture were distributed to each of four microcells and incubated for 10 min at 20ºC. The initial net NBD fluorescence intensity (F_0) was then determined by subtracting the signal of an equivalent NBD-free sample prepared with unmodified RTA from the NBD sample signal. Thereafter, each microcell received 10 µl of 2.0 M KCl, of 1.2 M KCl - 0.8 M KI, of 0.6 M KCl - 1.4 M KI, or of 2.0 M KI in the presence of 2 mM $Na_2S_2O_3$, and the net emission intensity of each sample (F) was measured. The ionic strength was therefore the same in each sample, but the iodide ion concentration differed. Thereafter, the microcells were incubated at 37ºC for 20 min and the net emission intensity of each sample was measured again. For steady state collisional quenching of fluorescence, a linear plot is obtained when the data are analyzed according to the Stern-Volmer law: $(F_0/F)-1 = K_{SV}[I]$ where K_{SV} is the Stern-Volmer quenching constant. K_{SV} is equal to $k_q\tau_0$, where k_q is the bimolecular quenching constant and τ_0 is the fluorescence lifetime in the absence of quencher.

Carbonate extraction- For carbonate extraction assays, $RTA^{259\text{-}NBD}$ (500 nM) and either KRMs (40 eq.) or PCPS-liposomes (2.5 mM) were incubated in buffer H for 30 min at 20ºC or 37ºC. Membranes were collected by sedimentation as before but at 15ºC. Following resuspension in ice cold carbonate buffer [0.1 M Na_2CO_3 (pH 11.5)] and incubation on ice for 15 min the membranes were collected by centrifugation at 4ºC, washed and recentrifuged before final resuspension in carbonate buffer. The combined supernatants of both centrifugation steps and the resupended pellets were neutralized with glacial acetic acid, and carrier BSA was added to a final concentration of 0.2 mg/mL. Proteins were precipitated with 12.5 % (w/v) TCA and further analyzed by SDS-PAGE. NBD-labeled proteins were visualized

using a fluorescence imager as above and protein band intensities were quantified using Quantity One Software V 4.6.5 (Bio-Rad). PC liposomes (5 mM) were incubated with $RTA^{259\text{-}NBD}$ (1 μM) in 10 mM HEPES (pH 7.5) for 30 min at either 20ºC or 37ºC. An equal volume of ice cold 0.2 M Na_2CO_3 (pH 11.5) was then added, and samples manipulated as described above.

In some experiments, carbonate buffer-treated KRMs were layered on a sucrose step gradient of 50% (60 μL) and 40% (80 μL) (w/v) sucrose in carbonate buffer and centrifuged (Beckman TLA100 rotor; 60,000 rpm; 30 min; 4ºC). The KRM layer was removed and collected by sedimentation as above. Following resuspension of the pellets in carbonate buffer, proteins were prepared for and analyzed by SDS-PAGE as above. Coomassie blue staining of the gel confirmed equal KRM recovery after the sucrose-step gradient purification (data not shown).

Preparation of fluorescent-labeled microsomes for FRET- To prepare rhodamine-labeled microsomes for FRET experiments, headgroup labeled rhodamine-phosphatidylethanolamine (Rh-PE, Avanti Polar Lipids) in chloroform was dried under a stream of nitrogen and further dried under vacuum for an additional 3 h. The Rh-PE film was hydrated in microsome buffer [50 mM triethanolamine (pH 7.5), 200 mM sucrose, 1 mM DTT] containing 250-400 equivalents (eq.) of KRMs to a final Rh-PE concentration of 2 μM and incubated for 1 h at 25ºC. The KRMs were then purified with a sucrose step gradient as decribed in text. The KRM layer was removed, and diluted with 2 volumes of buffer H. The KRMs were concentrated by sedimentation through a 0.5 M sucrose cushion in buffer H (Beckman TLA100.2 rotor; 60,000 rpm; 20 min; 4ºC), resuspended in buffer H, and aliquots were quick-frozen in liquid N_2 prior to storage at -80ºC.

FRET measurements- Four biochemically equivalent samples were prepared in parallel: sample D contained 65 nM $RTA^{259\text{-}NBD}$ adjusted to a total protein concentration of 560 nM with unlabeled RTA and unlabeled KRMs lacking Rh-PE; sample DA contained the same protein mixture as in D and Rh-PE•KRMs; sample A contained 560 nM unlabeled RTA and Rh-PE•KRMs; and sample B (blank) contained 560 nM unlabeled RTA and KRMs lacking Rh-PE. The KRM concentration was the same in all four samples, and the concentration of Rh-PE was the same in DA and A. The samples were incubated at 4ºC for 15 min before the initial spectral measurements were performed as described above. Thereafter, the temperature was increased to 37ºC for 20 min and a second set of measurements was performed. The net intensities of D (F_D), DA (F_{DA}), and A (F_A) were obtained by subtracting the B signal (F_B). To correct for any signal in the D sample caused by direct excitation of the acceptor, F_A was subtracted from F_{DA}. Since the presence of the acceptor dyes will not alter the donor dye absorbance, the efficiency of energy transfer, E, is given by $E = 1\text{-} (Q_{DA}/Q_D) = 1 - (\text{net } F_{DA} - \text{net } F_A)/\text{net } F_D$.

RESULTS

Temperature dependence of KRM membrane fluidity. To determine whether the ER membrane undergoes a phase change when the temperature is raised from 20ºC to 37ºC, we monitored KRM membrane fluidity by measuring the steady-state anisotropy of DPH that had been partitioned into the lipid phase of the ER membrane. As expected, the rotational rate of DPH was significantly slower (its anisotropy was higher) at 4ºC when embedded in the lipid bilayer ($r = 0.18$; Fig. S1) than when free in solution ($r = 0.01$). The anisotropy of KRM-incorporated DPH decreased as the temperature increased, consistent with a higher freedom of motion for the DPH probes due to enhanced membrane fluidity at higher temperatures. These results clearly show that the fluidity of the microsomal membrane is sensitive to the temperature. However, it is also clear that there is no sharp decrease in DPH anisotropy, and hence increase in membrane fluidity, between 20ºC and 37ºC. Given the absence of a dramatic phase change in the lipid bilayer between 30°C and 37°C, we conclude that the abrupt movement of the NBD dye at residue 259 of RTA from an aqueous milieu into the nonpolar membrane interior at that temperature did not result from a significant alteration in membrane fluidity or phase.

Intrinsic RTA fluorescence. When the temperature of an RTA sample was increased in small increments from 30ºC in the absence of

liposomes, a blue shift in $\lambda_{em\ max}$ was observed only above 41ºC (Fig. S2A), the temperature limit that is required for thermal unfolding of RTA (4). However, a Trp spectral shift was observed at 33–35ºC in the presence of PCPS liposomes (Fig. S2B).

Temperature dependence of iodide ion quenching of membrane-bound RTA$^{259\text{-}NBD}$. The accessibility of the NBD probes of RTA$^{259\text{-}NBD}$ to aqueous solvent was assessed by their sensitivity to collisional quenching by iodide ions. In the presence of microsomes, the reduction in RTA$^{259\text{-}NBD}$ NBD emission intensity yielded a K_{SV} of 5.5 ± 0.1 M^{-1} at 20ºC and a K_{SV} of 2.4 ± 0.3 M^{-1} at 37ºC (Fig. S3). In the absence of KRMs, the K_{SV} was 7.2 ± 0.4 M^{-1} at 20ºC (and 7.4 ± 0.8 at 37ºC, data not shown), consistent with a lower I^- accessibility to the NBD probe when RTA was bound to the membrane surface instead of free in solution. Since the quenching was directly proportional to the iodide ion concentration and yielded linear Stern-Volmer plots both in the presence and absence of KRMs, the observed quenching is collisional in nature.

The lipophilic quenching data (Fig. 5) and NBD emission spectra (Fig. 3) revealed that the NBD dye of membrane-bound RTA$^{259\text{-}NBD}$ moved from an aqueous to a more hydrophobic environment when the temperature was raised from 20ºC to 37ºC. The NBD dye has a short (1–2 ns) emission lifetime (τ) in aqueous solution and a longer lifetime (>6 ns) in a nonpolar environment (5,6). Since K_{SV} is equal to $k_q\tau_0$, the K_{SV} at 37ºC should have increased if the NBD probes had a longer lifetime and were still accessible to iodide ions. However, our experiments show the opposite: K_{SV} decreased at 37ºC. Thus, even without determining the fraction of buried NBD dyes at 37°C and measuring the NBD lifetimes at both 20°C and 37°C, the decreased K_{SV} at 37ºC can only be explained by a conformational change in membrane-bound RTA that moved the NBD to a location where it is inaccessible or less accessible to iodide ions, thereby reducing the collisional frequency between iodide ions and NBD dyes. The temperature-dependent aqueous and lipophilic quenching data therefore complement and reinforce each other, since these combined data show that NBD dyes simultaneously enter the nonpolar core of the bilayer and leave the aqueous solvent when the temperature reaches 37°C. Hence, the combined results strongly support the view that at 37°C a protein conformational change at the C-terminus of RTA moves C259 from an aqueous-exposed site on the RTA surface to a location at the membrane surface that is exposed to the interior.

RTA proximity to the membrane surface. The temperature dependence of the spectral changes suggests that RTA undergoes a conformational change after binding to the membrane surface. To detect experimentally whether such a change occurs, we have used a variation of the fluorescence resonance energy transfer (FRET) technique to assess the proximity of the NBD at Cys259 to the membrane surface.

In a typical FRET experiment, an excited fluorescent dye (the donor) transfers its excited state energy to a second dye or chromophore (the acceptor) with the appropriate spectral properties. The efficiency of this energy transfer, E, depends on several variables, but most importantly on the distance between the donor and acceptor dyes. Thus, FRET is generally used to measure point-to-point inter- or intra-molecular distances between a donor dye and an acceptor dye located at specific sites (1,7,8). However, a variation of the FRET technique quantifies the distance of closest approach (L) between donor dyes attached to membrane-bound proteins and acceptor dyes localized at the membrane surface, thereby measuring the height of the protein-bound dye above the membrane surface (7,9-12). In this approach, the extent of energy transfer observed in a particular experiment depends directly on the surface density and distribution of the acceptor dyes at the membrane surface. Here, the donor was NBD in RTA$^{259\text{-}NBD}$. The acceptor dye, rhodamine, was covalently attached to a phosphatidylethanolamine headgroup to form Rh-PE, thereby ensuring that the acceptor is localized at the membrane surface. The acceptor was introduced into ER membranes by fusing micelles of Rh-PE with microsomes, after which Rh-PE then diffuses throughout the bulk lipid on the cytoplasmic leaflet of the microsomal membrane (B. Hou, personal communication).

To properly determine E for RTA$^{259\text{-}NBD}$ bound to Rh-PE•KRMs, four separate samples must be prepared that are identical except for the presence or absence of the donor and/or acceptor dyes. Thus, the D sample contained RTA$^{259\text{-}NBD}$

and KRMs, the DA sample contained $RTA^{259\text{-}NBD}$ and Rh-PE•KRMs, the A sample contained RTA and Rh-PE•KRMs, and the B (blank) sample contained RTA and KRMs. E was then determined by the magnitude of the acceptor-dependent decrease in donor emission intensity (9,11-13).

When $RTA^{259\text{-}NBD}$ was incubated with Rh-PE•KRMs at 4ºC, we found that E was 3 ± 1%. In contrast, when the same sample was then incubated at 37ºC, E increased to 25 ± 1 %. Since the above gel filtration, sedimentation (Fig. 1), and anisotropy data (Fig. 2) showed that RTA binds to KRMs at all temperatures examined (0ºC - 37ºC), this result reveals directly that the NBD at Cys259 moves closer to the membrane surface at 37ºC. At 4ºC, the NBD dyes are located further from the membrane surface. [This change in FRET efficiency is too large to be explained solely be an alteration in the relative orientation of the donor and acceptor transition dipoles because of the small change in NBD anisotropy that occurs when the temperature is increased from 4°C to 37°C (Fig. 2A) and the fact that the Rh-PE dyes are randomly oriented at the membrane surface.] The high density of ER membrane proteins and the possibility of lipid microdomains in the microsomal membrane make it impossible to determine experimentally the density and uniformity of distribution of the acceptor dyes at the surface. Therefore, we cannot calculate the exact height of the NBD dye above the membrane surface for these natural membranes. However, the critical issue is not the magnitude of this height, but rather whether this distance changes as the temperature is increased from 4ºC to 37ºC. The fact that the FRET efficiency differs at 4ºC and 37ºC shows that the spatial separation of the C-terminus of RTA from the membrane surface at 4ºC is reduced when the temperature is raised to 37ºC.

Fluorescence properties of NBD probes at different sites in RTA derivatives. RTAs with NBD probes positioned at different sites in the protein were used to assess the extent of the membrane binding-dependent conformational changes. To covalently attach NBD to the single-Lys RTA derivatives, a seven-atom aminohexanoyl spacer between NBD and the protein was used. Because this dye tether was longer than that of the Cys mutants, the Lys mutants had lower anisotropy values than did the Cys-labeled variants (Table S1). Yet the binding of each derivative to microsomes at 37ºC was shown by an increase in its NBD anisotropy (Table S2).

REFERENCES

1. Johnson, A. E., Adkins, H. J., Matthews, E. A., and Cantor, C. R. (1982) *J Mol Biol* **156**(1), 113-140
2. Haugland, R. P. (2002) *Handbook of fluorescent probes and research products*, 9 Ed., Molecular Probes, Inc., Eugene, OR
3. Heuck, A. P., Tweten, R. K., and Johnson, A. E. (2003) *J Biol Chem* **278**(33), 31218-31225
4. Argent, R. H., Parrott, A. M., Day, P. J., Roberts, L. M., Stockley, P. G., Lord, J. M., and Radford, S. E. (2000) *J Biol Chem* **275**(13), 9263-9269
5. Crowley, K. S., Reinhart, G. D., and Johnson, A. E. (1993) *Cell* **73**(6), 1101-1115
6. Shepard, L. A., Heuck, A. P., Hamman, B. D., Rossjohn, J., Parker, M. W., Ryan, K. R., Johnson, A. E., and Tweten, R. K. (1998) *Biochemistry* **37**(41), 14563-14574
7. Johnson, A. E. (2005) *Traffic* **6**(12), 1078-1092
8. Woolhead, C. A., McCormick, P. J., and Johnson, A. E. (2004) *Cell* **116**(5), 725-736
9. Ramachandran, R., Tweten, R. K., and Johnson, A. E. (2005) *Proc Natl Acad Sci U S A* **102**(20), 7139-7144
10. Yegneswaran, S., Smirnov, M. D., Safa, O., Esmon, N. L., Esmon, C. T., and Johnson, A. E. (1999) *J Biol Chem* **274**(9), 5462-5468
11. Husten, E. J., Esmon, C. T., and Johnson, A. E. (1987) *J Biol Chem* **262**(27), 12953-12961
12. Mutucumarana, V. P., Duffy, E. J., Lollar, P., and Johnson, A. E. (1992) *J Biol Chem* **267**(24), 17012-17021
13. Yegneswaran, S., Wood, G. M., Esmon, C. T., and Johnson, A. E. (1997) *J Biol Chem* **272**(40), 25013-25021

FIGURE LEGENDS

Fig. S1. KRM membrane fluidity. DPH was incorporated into the KRMs (20 eq.) as described in Experimental Procedures and its steady-state anisotropy (◆) was determined as a function of temperature in buffer H. Anisotropy data were corrected by the subtraction of the signal obtained from an equivalent DPH-free KRM sample. The anisotropy of free DPH (○) was determined using methanol as solvent in a sample lacking KRMs. The averages of at least three independent experiments are shown, and the error bars indicate the S.D. of the experiments. However, most error bars are smaller than the circles on the graph.

Fig. S2. Temperature dependence of RTA binding to liposomes. Intrinsic Trp emission spectra of RTA [7 μM in buffer C in the absence (*A*) or presence (*B*) of 200 μM PCPS liposomes] were measured (λ_{ex} = 280 nm). The temperature was increased stepwise and an emission scan was recorded after 10 min of equilibration.

Fig. S3. Temperature dependence of iodide ion quenching of KRM-bound $RTA^{259\text{-}NBD}$. $RTA^{259\text{-}NBD}$ (450 nM) and either KRMs (80 eq.; ●; ■) or an equal volume of microsome buffer (○) were combined in 1200 μl buffer H, split into four aliquots, incubated for 10 min at 20ºC, and the initial net emission intensity (F_0) of each aliquot was measured. Different amounts of KI were then added to each sample, along with sufficient KCl to keep the ionic strength the same for each aliquot, and the emission intensities (F) were measured at 20ºC (○;●). Thereafter, the samples were incubated for 20 min at 37ºC, and the emission intensities were measured again (■). K_{SV} values were determined by a linear least square analysis of the combined data of three independent experiments.

Fig. S4. CD-detected RTA conformation is PS dependent. The far UV CD signal changes at 208 nm of RTA [5 μM in buffer C] with increasing temperature in the absence and presence of 200 μM liposomes containing different percentages of PS are shown. The temperature was increased at 1ºC/min and the signal was measured every minute. Data from at least two independent experiments were averaged.

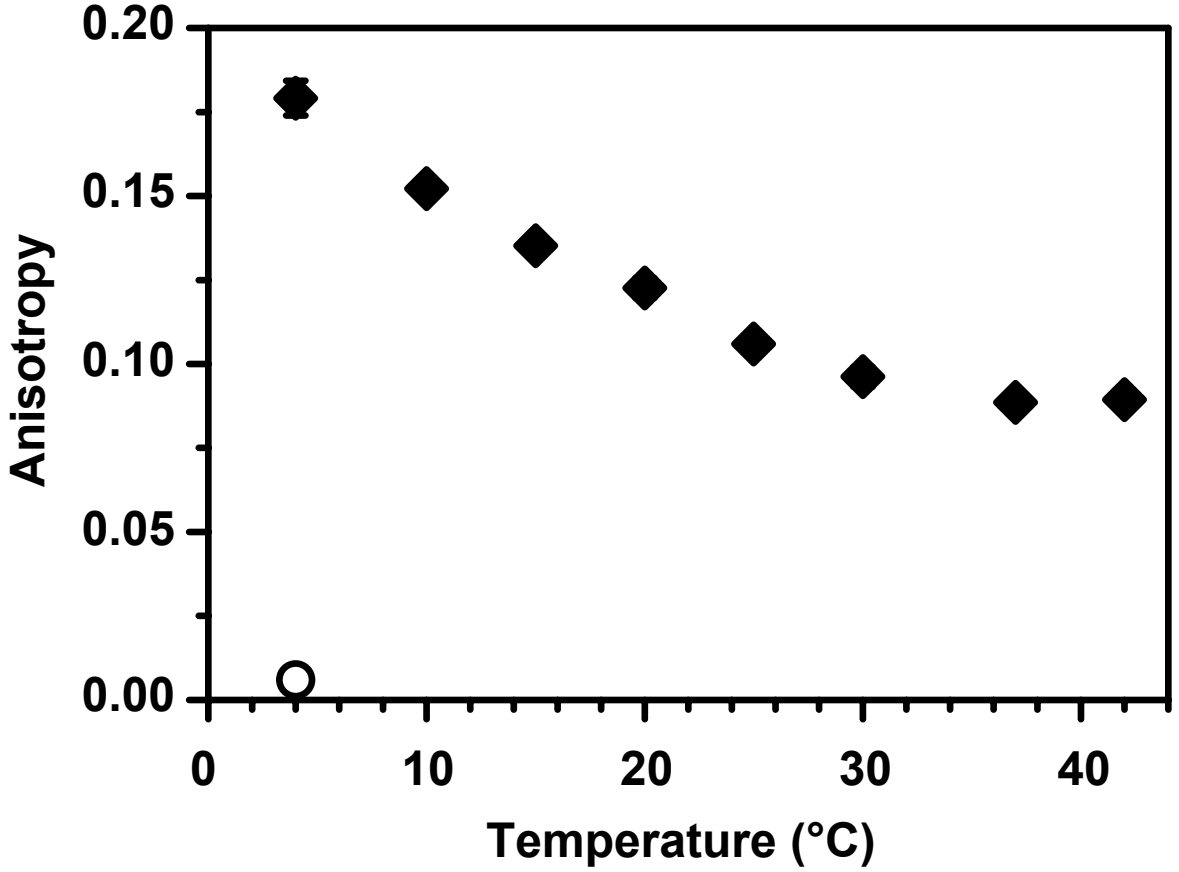

Figure S1

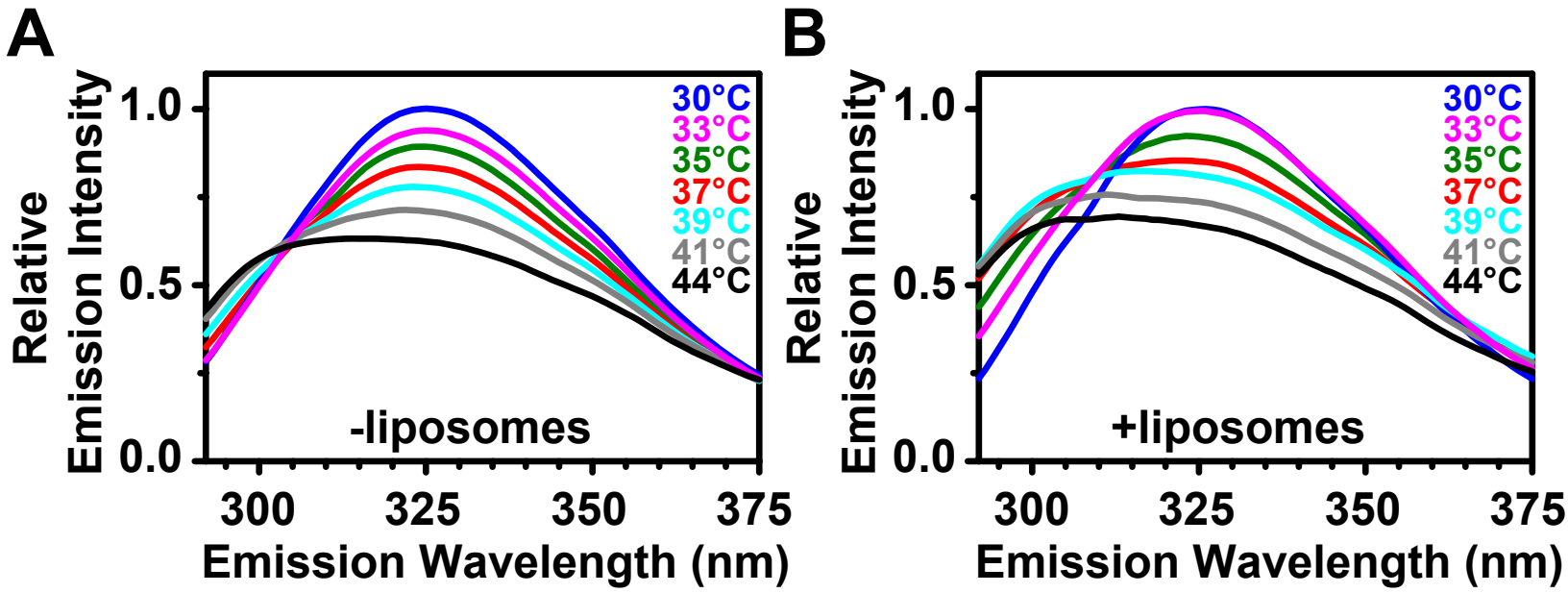
A
B
Relative Emission Intensity
1.0
0.5
0.0
30°C
33°C
35°C
37°C
39°C
41°C
44°C
-liposomes
+liposomes
300
325
350
375
Emission Wavelength (nm)

Figure S2

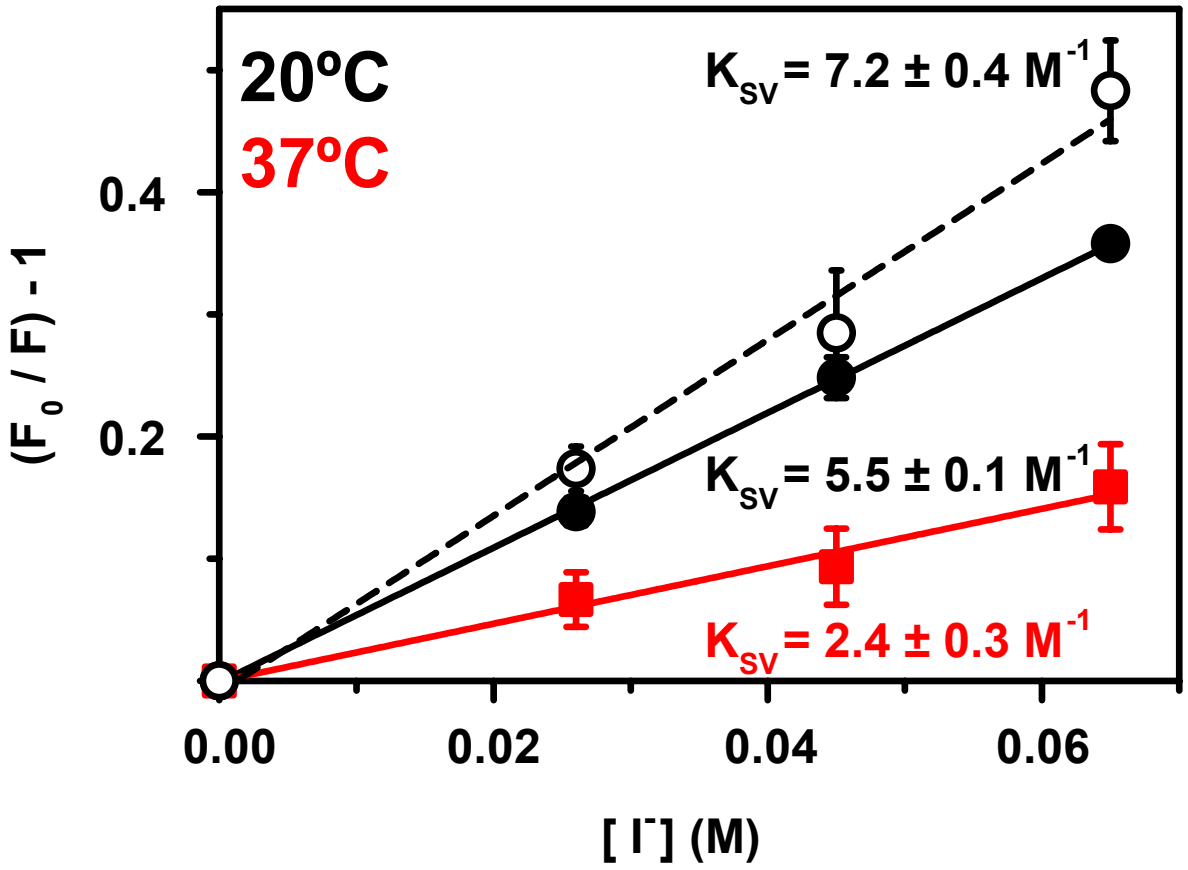
20ºC
37ºC
K_{SV} = 7.2 ± 0.4 M^{-1}
K_{SV} = 5.5 ± 0.1 M^{-1}
K_{SV} = 2.4 ± 0.3 M^{-1}
$(F_0 / F) - 1$
0.4
0.2
0.00
0.02
0.04
0.06
[I^-] (M)

Figure S3

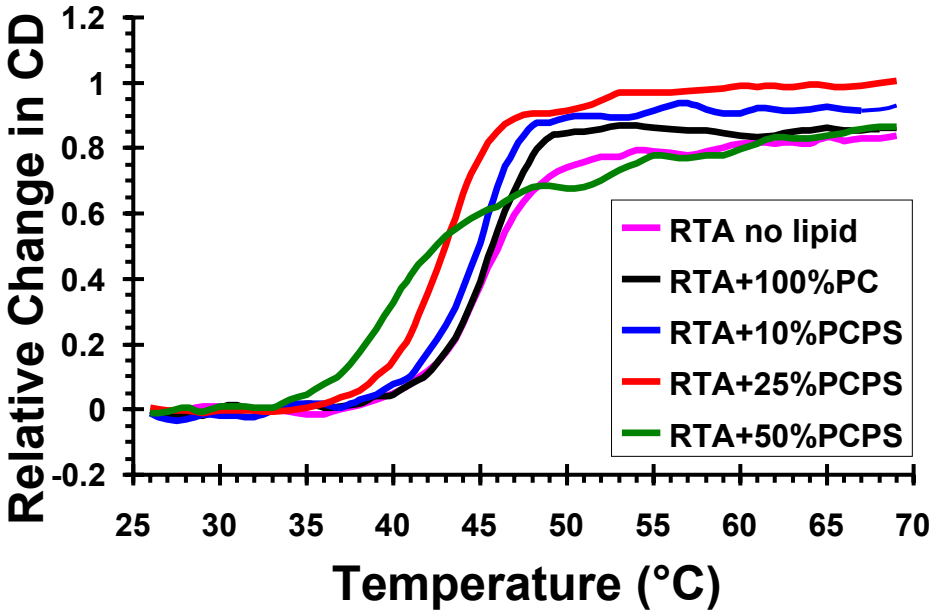
Relative Change in CD
1.2
1
0.8
0.6
0.4
0.2
0
-0.2
25
30
35
40
45
50
55
60
65
70
Temperature (°C)
RTA no lipid
RTA+100%PC
RTA+10%PCPS
RTA+25%PCPS
RTA+50%PCPS

Figure S4

Table S1: Fluorescence properties of NBD probes at different sites in soluble RTA proteins

	soluble			
	$\lambda_{em\ max}$		anisotropy	
RTA derivative	20ºC	37ºC	20ºC	37ºC
$RTA^{31\text{-}NBD}$	544 ± 1	542 ± 3	0.169 ± 0.002	0.150 ± 0.037
$RTA^{61\text{-}NBD}$	542 ± 2	537 ± 2	0.162 ± 0.007	0.150 ± 0.015
$RTA^{98\text{-}NBD}$	546 ± 2	543 ± 2	0.127 ± 0.007	0.121 ± 0.008
$RTA^{114\text{-}NBD}$	544 ± 2	542 ± 3	0.132 ± 0.004	0.150 ± 0.029
$RTA^{128\text{-}NBD}$	544 ± 3	538 ± 3	0.143 ± 0.014	0.167 ± 0.017
$RTA^{135\text{-}NBD}$	540 ± 2	539 ± 2	0.129 ± 0.002	0.153 ± 0.016
$RTA^{249\text{-}NBD}$	537 ± 2	537 ± 2	0.267 ± 0.013	0.295 ± 0.003
$RTA^{259\text{-}NBD}$	540 ± 1	540 ± 1	0.249 ± 0.009	0.237 ± 0.004

Emission scans (λ_{ex} = 468 nm) and anisotropy measurements of NBD-labeled RTA derivatives [450 nM in buffer H] were performed at either 20ºC or 37ºC. Emission intensity and anisotropy data were corrected by the subtraction of the signal obtained form an equivalent NBD-free RTA sample. The averages and S.D. of at least three independent experiments are shown.

.

Table S2: Fluorescence properties of NBD probes at different sites in membrane-bound RTA proteins

	membrane-bound			
	$\lambda_{em\ max}$		anisotropy	
RTA derivative	20ºC	37ºC	20ºC	37ºC
$RTA^{31\text{-}NBD}$	540 ± 2	533 ± 3	0.213 ± 0.008	0.220 ± 0.009
$RTA^{61\text{-}NBD}$	529 ± 1	533 ± 1	0.263 ± 0.014	0.223 ± 0.016
$RTA^{98\text{-}NBD}$	538 ± 1	535 ± 2	0.207 ± 0.033	0.235 ± 0.010
$RTA^{114\text{-}NBD}$	535 ± 1	539 ± 3	0.220 ± 0.013	0.186 ± 0.036
$RTA^{128\text{-}NBD}$	543 ± 1	536 ± 3	0.252 ± 0.014	0.217 ± 0.034
$RTA^{135\text{-}NBD}$	542 ± 2	536 ± 2	0.194 ± 0.044	0.224 ± 0.046
$RTA^{249\text{-}NBD}$	536 ± 1	529 ± 2	0.298 ± 0.020	0.333 ± 0.002
$RTA^{259\text{-}NBD}$	539 ± 3	526 ± 1	0.307 ± 0.017	0.293 ± 0.004

Emission scans (λ_{ex} = 468 nm) and anisotropy measurements of NBD-labeled RTA derivatives [450 nM in buffer H] were performed after addition of KRMs (20 eq.) at either 20ºC or 37ºC. Emission intensity and anisotropy data were corrected by the subtraction of the signal obtained form an equivalent NBD-free RTA sample. The averages and S.D. of at least three independent experiments are shown.